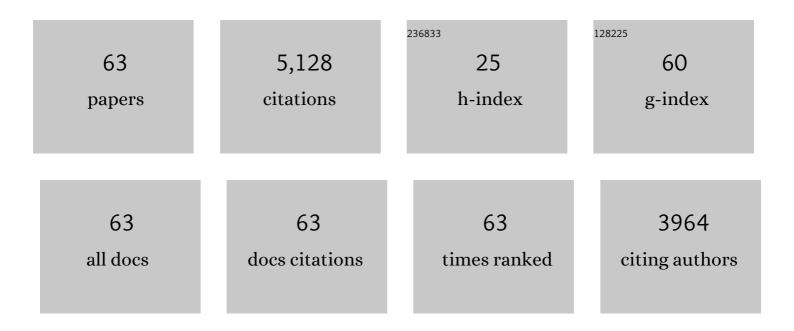
## Diana Berman

List of Publications by Year in descending order

Source: https://exaly.com/author-pdf/6855421/publications.pdf Version: 2024-02-01



#	Article	IF	CITATIONS
1	Graphene: a new emerging lubricant. Materials Today, 2014, 17, 31-42.	8.3	1,115
2	Macroscale superlubricity enabled by graphene nanoscroll formation. Science, 2015, 348, 1118-1122.	6.0	665
3	Few layer graphene to reduce wear and friction on sliding steel surfaces. Carbon, 2013, 54, 454-459.	5.4	607
4	Reduced wear and friction enabled by graphene layers on sliding steel surfaces in dry nitrogen. Carbon, 2013, 59, 167-175.	5.4	417
5	Approaches for Achieving Superlubricity in Two-Dimensional Materials. ACS Nano, 2018, 12, 2122-2137.	7.3	364
6	Extraordinary Macroscale Wear Resistance of One Atom Thick Graphene Layer. Advanced Functional Materials, 2014, 24, 6640-6646.	7.8	251
7	Operando tribochemical formation of onion-like-carbon leads to macroscale superlubricity. Nature Communications, 2018, 9, 1164.	5.8	199
8	Nanoscale friction properties of graphene and graphene oxide. Diamond and Related Materials, 2015, 54, 91-96.	1.8	108
9	Surface science, MEMS and NEMS: Progress and opportunities for surface science research performed on, or by, microdevices. Progress in Surface Science, 2013, 88, 171-211.	3.8	101
10	Sequential Infiltration Synthesis for the Design of Low Refractive Index Surface Coatings with Controllable Thickness. ACS Nano, 2017, 11, 2521-2530.	7.3	84
11	Layered 2D Nanomaterials to Tailor Friction and Wear in Machine Elements—A Review. Advanced Materials Interfaces, 2022, 9, .	1.9	80
12	Graphene as a protective coating and superior lubricant for electrical contacts. Applied Physics Letters, 2014, 105, .	1.5	75
13	Inhibitor or promoter: Insights on the corrosion evolution in a graphene protected surface. Carbon, 2018, 126, 225-231.	5.4	72
14	Metal-induced rapid transformation of diamond into single and multilayer graphene on wafer scale. Nature Communications, 2016, 7, 12099.	5.8	70
15	Micro-/Nanotopography on Bioresorbable Zinc Dictates Cytocompatibility, Bone Cell Differentiation, and Macrophage Polarization. Nano Letters, 2020, 20, 4594-4602.	4.5	55
16	Operando formation of an ultra-low friction boundary film from synthetic magnesium silicon hydroxide additive. Tribology International, 2017, 110, 35-40.	3.0	53
17	The Structure of Amorphous and Deeply Supercooled Liquid Alumina. Frontiers in Materials, 2019, 6, .	1.2	51
18	Discontinuous fatty acid elongation yields hydroxylated seed oil with improved function. Nature Plants, 2018, 4, 711-720.	4.7	43

DIANA BERMAN

#	Article	IF	CITATIONS
19	Achieving Ultralow Friction and Wear by Tribocatalysis: Enabled by <i>In-Operando</i> Formation of Nanocarbon Films. ACS Nano, 2021, 15, 18865-18879.	7.3	42
20	Ironâ€Nanoparticle Driven Tribochemistry Leading to Superlubric Sliding Interfaces. Advanced Materials Interfaces, 2019, 6, 1901416.	1.9	41
21	Effect of trapped water on the frictional behavior of graphene oxide layers sliding in water environment. Carbon, 2017, 120, 11-16.	5.4	35
22	Impact of oxygen and argon plasma exposure on the roughness of gold film surfaces. Thin Solid Films, 2012, 520, 6201-6206.	0.8	34
23	Nature-Guided Synthesis of Advanced Bio-Lubricants. Scientific Reports, 2019, 9, 11711.	1.6	33
24	Combined Tribological and Bactericidal Effect of Nanodiamonds as a Potential Lubricant for Artificial Joints. ACS Applied Materials & Interfaces, 2019, 11, 43500-43508.	4.0	30
25	Design of functional composite and all-inorganic nanostructured materials <i>via</i> infiltration of polymer templates with inorganic precursors. Journal of Materials Chemistry C, 2020, 8, 10604-10627.	2.7	29
26	Self-healing ceramic coatings that operate in extreme environments: A review. Journal of Vacuum Science and Technology A: Vacuum, Surfaces and Films, 2020, 38, .	0.9	28
27	Dramatic Enhancement of Optoelectronic Properties of Electrophoretically Deposited C <sub>60</sub> –Graphene Hybrids. ACS Applied Materials & Interfaces, 2019, 11, 24349-24359.	4.0	27
28	PEO-Chameleon as a potential protective coating on cast aluminum alloys for high-temperature applications. Surface and Coatings Technology, 2020, 397, 126016.	2.2	27
29	Rapid Synthesis of Nanoporous Conformal Coatings via Plasma-Enhanced Sequential Infiltration of a Polymer Template. ACS Omega, 2017, 2, 7812-7819.	1.6	23
30	Block-Co-polymer-Assisted Synthesis of All Inorganic Highly Porous Heterostructures with Highly Accessible Thermally Stable Functional Centers. ACS Applied Materials & Interfaces, 2019, 11, 30154-30162.	4.0	22
31	Effect of Water Incorporation on the Lubrication Characteristics of Synthetic Oils. Tribology Letters, 2019, 67, 1.	1.2	21
32	Accessibility of the pores in highly porous alumina films synthesized via sequential infiltration synthesis. Nanotechnology, 2018, 29, 495703.	1.3	19
33	Nanodiamonds for improving lubrication of titanium surfaces in simulated body fluid. Carbon, 2019, 143, 890-896.	5.4	19
34	Electrical Contact Resistance and Device Lifetime Measurements of Au-RuO2-Based RF MEMS Exposed to Hydrocarbons in Vacuum and Nitrogen Environments. Tribology Letters, 2011, 44, 305-314.	1.2	18
35	Electrospun Fe3O4-PVDF Nanofiber Composite Mats for Cryogenic Magnetic Sensor Applications. Textiles, 2021, 1, 227-238.	1.8	18
36	Silica nanoparticles as copper corrosion inhibitors. Materials Research Express, 2019, 6, 0850e3.	0.8	17

DIANA BERMAN

#	Article	IF	CITATIONS
37	Substrate effect on electrical conductance at a nanoasperity-graphene contact. Carbon, 2018, 137, 118-124.	5.4	16
38	TiCaPCON-Supported Pt- and Fe-Based Nanoparticles and Related Antibacterial Activity. ACS Applied Materials & amp; Interfaces, 2019, 11, 28699-28719.	4.0	16
39	Effect of the Micelle Opening in Self-assembled Amphiphilic Block Co-polymer Films on the Infiltration of Inorganic Precursors. Langmuir, 2019, 35, 796-803.	1.6	16
40	Laser surface modification of porous yttria stabilized zirconia against CMAS degradation. Ceramics International, 2020, 46, 6038-6045.	2.3	16
41	Magnesium Silicate Hydroxide–MoS <sub>2</sub> –Sb <sub>2</sub> O <sub>3</sub> Coating Nanomaterials for High-Temperature Superlubricity. ACS Applied Nano Materials, 2021, 4, 7097-7106.	2.4	16
42	Tribologically enhanced self-healing of niobium oxide surfaces. Surface and Coatings Technology, 2019, 364, 273-278.	2.2	15
43	Macroscale Superlubricity Accomplished by Sb2O3-MSH/C Under High Temperature. Frontiers in Chemistry, 2021, 9, 667878.	1.8	15
44	Tribocatalytically-activated formation of protective friction and wear reducing carbon coatings from alkane environment. Scientific Reports, 2021, 11, 20643.	1.6	14
45	Effect of Substrate Support on Dynamic Graphene/Metal Electrical Contacts. Micromachines, 2018, 9, 169.	1.4	11
46	Lubrication characteristics of wax esters from oils produced by a genetically-enhanced oilseed crop. Tribology International, 2020, 146, 106234.	3.0	10
47	Swelling-Assisted Sequential Infiltration Synthesis of Nanoporous ZnO Films with Highly Accessible Pores and Their Sensing Potential for Ethanol. ACS Applied Materials & Interfaces, 2021, 13, 35941-35948.	4.0	10
48	Impact of adsorbed organic monolayers on vacuum electron tunneling contributions to electrical resistance at an asperity contact. Journal of Applied Physics, 2011, 110, .	1.1	9
49	Canted antiferromagnetism in the quasi-one-dimensional iron chalcogenide <mmi:math xmlns:mml="http://www.w3.org/1998/Math/MathML"&gt; <mmi:msub> <mmi:mi mathvariant="normal"&gt;BaFe <mmi:mn>2</mmi:mn> </mmi:mi </mmi:msub> <mmi:msub> <mmi:mi mathvariant="normal"&gt;Se <mmi:mn>4</mmi:mn> </mmi:mi </mmi:msub> . Physical Review B,</mmi:math 	1.1	9
50	2020, 102. Hydrogen generating patch improves skin cell viability, migration activity, and collagen expression. Engineered Regeneration, 2020, 1, 1-5.	3.0	9
51	Method for tribological experiment to study scuffing initiation on AISI 52100 steel and hard ceramic coatings. Tribology International, 2021, 160, 107001.	3.0	9
52	Oxidation-induced healing in laser-processed thermal barrier coatings. Thin Solid Films, 2019, 688, 137481.	0.8	8
53	Al/Al2O3 metal matrix composites produced using magnetic field-assisted freeze-casting of porous ceramic structures. Journal of Materials Research, 2021, 36, 2094-2106.	1.2	7
54	Controlling anisotropy of porous B4C structures through magnetic field-assisted freeze-casting. Ceramics International, 2022, 48, 6750-6757.	2.3	7

DIANA BERMAN

#	Article	IF	CITATIONS
55	Mechanical and chemical robustness of the aluminum oxide-infiltrated block copolymer films and the resulting aluminum oxide coatings. Surface and Coatings Technology, 2020, 399, 126204.	2.2	5
56	Design of porous aluminum oxide ceramics using magnetic field-assisted freeze-casting. Journal of Materials Research, 2020, 35, 2859-2869.	1.2	4
57	A comparative study of calcium–magnesium–aluminum–silicon oxide mitigation in selected self-healing thermal barrier coating ceramics. Journal of Materials Research, 2020, 35, 2311-2320.	1.2	4
58	Observation of room-temperature superparamagnetic behavior of Fe5Si3 nanocrystals synthesized via 50ÂkeV Fe ion implantation in silicon. Applied Physics A: Materials Science and Processing, 2020, 126, 1.	1.1	3
59	Effect of Polymer Removal on the Morphology and Phase of the Nanoparticles in All-Inorganic Heterostructures Synthesized via Two-Step Polymer Infiltration. Molecules, 2021, 26, 679.	1.7	3
60	Thermal stability and gas absorption characteristics of ionic liquid-based solid polymer electrolytes. Journal of Chemical Physics, 2021, 154, 054902.	1.2	3
61	Graphene: Extraordinary Macroscale Wear Resistance of One Atom Thick Graphene Layer (Adv. Funct.) Tj ETQq1	1 0.78431 7.8	4 rgBT /Ove
62	Friction and Wear of Carbon-Containing Composites. , 2017, , 550-558.		0
63	Chinese Violet Cress: Novel Seed Oil Biosynthesis, Storage, and Functionality. , 0, , .		0